Peer-reviewed version available at *Polymers* **2017**, *9*, 688; doi:10.3390/polym9120688

Article

Thermal conduction behaviors of PAAm hydrogels

Ni Tang[1,†], Zhan Peng[3,4,†], Rulei Guo[3,4,†], Meng An[3,4], Xiandong Chen[3,4], Xiaobo Li[3,4], Nuo Yang[3,4] ' *and Jianfeng Zang[1,2,*]

[1] School of Optical and Electronic Information, Huazhong University of Science and Technology, 1037 Luoyu Rd., 430074 Wuhan, China; minnie_tang@hust.edu.cn (N.T.)

2 Innovation Institute, Huazhong University of Science and Technology, 1037 Luoyu Rd., 430074 Wuhan, China

[3] Key Laboratory of Coal Combustion, Huazhong University of Science and Technology, 1037 Luoyu Rd., 430074 Wuhan, China; pengzhanhust@qq.com (Z.P.); guorulei@hust.edu.cn (R.G.); anmeng@hust.edu.cn (M.A.); xiandongchen@qq.com (X.C.); xbli35@hust.edu.cn (X.L.)

[4] Nano Interface Center for Energy, School of Energy and Power Engineering Huazhong University of Science and Technology, 1037 Luoyu Rd., 430074 Wuhan, China

* Correspondence: jfzang@hust.edu.cn (J.Z.); nuo@hust.edu.cn (Y.N.); Tel: +86-

† These authors contributed equally to this work.

Abstract: As the interface between human and machine becomes blurred, hydrogel incorporated electronics and devices have emerged to be a new class of flexible/stretchable electronic and ionic devices due to their extraordinary properties, such as soft, mechanically robust and biocompatible. However, heat dissipation in these devices could be a critical issue and remains unexplored. Here, we report the experimental measurements and equilibrium molecular dynamics simulations of thermal conduction in polyacrylamide (PAAm) hydrogels. The thermal conductivity of PAAm hydrogels can be modulated by both the crosslinking density and water content in hydrogels. The crosslinking density dependent thermal conductivity in hydrogels varies from 0.33 to 0.51 $Wm^{-1}K^{-1}$, giving a 54% enhancement. We attribute the crosslinking effect to the competition between the increased conduction pathways and the enhanced phonon scattering effect. Moreover， water content can act as filler in polymers which lead to nearly 40% enhancement in thermal conductivity in PAAm hydrogels with water content vary from 23 to 88 wt%. Furthermore， we find the thermal conductivity of PAAm hydrogel is insensitive to temperature in the range of 25 °C – 40 °C. Our study offers fundamental understanding of thermal transport in soft materials and provides design guidance for hydrogel-based devices.

Keywords: hydrogel; thermal conductivity; 3ω method; molecular dynamics

1. Introduction

Human bodies are mainly composed of soft hydrogels, such as living tissues and muscles. Hydrogels are regarded as one big molecule on macroscale with cross-linked polymer network containing significant amounts of water (70-99 wt %)[1]. These intrinsic half-liquid and half-solid characteristics bring hydrogels broad applications such as tissue engineering[2], cell encapsulation[3], drug delivery[4], and soft actuators[1]. Addition to above traditional applications, the emerging hydrogel-based applications are focused on soft electronics, soft robotics and machines[5]. Most applications involving grasping, movement and swelling, thus numerous studies

have been carried out to enhance their mechanical properties, such as stretchability, young's modulus, and fracture energy[6–10].

Besides mechanical properties, heat dissipation in hydrogel-based electronic devices, as well as soft electronics, however, remains largely unexplored, which may be arisen from the fact that hydrogels used in above domains usually fulfill simple actions based on environmental sensitivity without much participating of electronic component. While for more sophisticated applications, some energy consuming electronic components and devices, such as conductive wires, rigid electronic devices, and other functional components will be involved in biocompatible, soft while mechanically robust hydrogels[9]. More inspiring examples include ionic hydrogel-based highly stretchable and transparent touch panel[11], the steerable smart catheter tip realized by flexible hydrogel actuator[12], double-networking hydrogel-based optical fibers for strain sensors[13] and so on. The attempt on the integration of soft hydrogels with rigid machines shows prominent potential to revolutionize flexible electronics, soft robotics and even medical technologies. The possible heat dissipation at the hydrogel-machine interface with encapsulated electronics components could be a serious issue and need a better understanding.

Existing thermal studies involving hydrogels mainly focused on their nanocomposites and their thermal stabilities[14–17] and thermal diffusivity[18], but not on pure hydrogels and their thermal transportation properties. The hydrogel nanocomposites incorporated with boron nitride (BN) nanopalettes shows an enhanced thermo-responsive time in poly(N -isopropyl- acrylamide) (PNIPAm)/BN hydrogels or a better performance as thermal interface materials in poly(acrylic acid) (PAA)/BN hydrogels[19,20]. These investigations pay attention to the role of nanofillers, a compelling experimental investigation of intrinsic thermal conductivity of hydrogels itself has not yet been well explored.

Here, we report the first experimental investigation of thermal conduction in hydrogels. The polyacrylamide (PAAm) hydrogel is chosen as a model hydrogel since PAAm is popular for soft electronics and ionic conductors. Both the experimental and simulation results show that the thermal conductivity have an obvious dependence on crosslinking concentrations, which is regarded as a key factor for hydrogels' mechanical properties[10]. The resultant thermal conductivities of PAAm are in a range of 0.33±0.06 ~ 0.51± 0.03 $Wm^{-1}K^{-1}$, which is slightly below the thermal conductivity of pure water (~0.6 $Wm^{-1}K^{-1}$). We explore the thermal conduction mechanism in hydrogels through equilibrium swelling ratio measurements, scanning electron microscope (SEM) characterization and equilibrium molecular dynamic (EMD) simulation. The thermal stability of hydrogel with its water content and environment temperature effects has also been evaluated. Our study on the thermal conduction behavior in hydrogels may potentially impact in both traditional biomedical field as well as the emerging soft electronics.

2. Materials and Methods

2.1. Materials Synthesis

All the following reagents were purchased from Sinopharm Chemical Reagent Co., Ltd. and used without further modified. As prepared PAAm hydrogels are clear and transparent as shown in Figure 1a PAAm are made from acrylamide (AAm) monomers consisting of carbon double bond and the $–CONH_2$ group, which could be co-polymerized by crosslinkers, e.g., N–methylenebisacrylamide (MBAm), as shown in Figure 1b and 1c.

Samples were synthesized by standard free radicals copolymerization method[7]. AAm powders were dissolved in deionized water (12 wt %) and mixed with different molar ratio of MBAm as a cross-linker. Ammonium persulfate (APS) in water (3 wt %) as initiator and N, N, N′, N′-tetramethylethylenediamine (TEMED) as the crosslinking accelerator were added into the above solution in sequence. The gel was then sealed under humid condition for future use.

2.2 3ω Method

When an AC electrical current at angular frequency 1ω is applied at two electrodes, a small voltage signal across the heater to another two electrodes could be detected. The voltage at a frequency of 3ω carrying the thermal effect signal is selected. Combining the relationship among the frequency, voltage and temperature enhancement, the thermal properties of hydrogels can be extracted. Thus, this class of measurement is aptly known as "3ω" method.

Figure 1d presents the schematic diagram of our experimental setup of 3ω method for the crosslinking density dependent thermal conduction measurement of the hydrogels. A platinum wire with a diameter of 1 mm connected by four copper electrode rods is immersed in hydrogels. The Pt wire serves as both heater and thermometer. The photo of the real setup and an example for detailed data analysis to obtain the thermal conductivity is shown in Figure S1and S2 (Supplementary Information) accordingly.

For measurement of influence of water content and temperature on thermal conductivity of PAAm hydrogels, the setups (Figure S3, Supplementary Information) differ from that of crosslinking density dependent thermal conduction measurement owing to the fragile heaters would be ruptured when volume of PAAm change by its deswelling in ethanol solution, and the convenience to apply higher temperature to samples, accordingly. More details on the description of 3ω method can be found in the Supporting Information.

The feasibility of our measurement setup is validated with test of deionized water at room temperature. The measured thermal conductivity of deionized water is 0.60 $Wm^{-1}K^{-1}$, which shows a good agreement with the data in NIST database REFPROP. Multiple measurements were conducted on every hydrogel sample to ensure the reliability and reproducibility of our results.

2.3 Equilibrium swelling ratio measurement

For the equilibrium swelling measurements, PAAm gels with different crosslinker concentrations were cut into the same cylinder shape (1 cm in diameter, 3 cm in length). Then, we dry these samples to constant weight in a vacuum oven. To obtain the equilibrium swelling ratio, dry samples were soaked in deionized (DI) water till they reached maximum weight. The weights of the samples as a function of time are recorded.

2.4 EMD simulation

Atomistic simulations provide a powerful tool for validation and interpretation of experimental results[21]. We have performed EMD simulations of thermal transport in hydrogels with different crosslinking concentrations. In experimental measurements, the weight ratio of water in hydrogel samples with different crosslinking concentrations keeps unchanged. In simulations, to simplify the case, we ignore water effect in hydrogels and only consider PAAm and MBAm. The crosslinking density (MBAm) is set from 0.0017 mol % to 0.17 mol % at 300 K. All the simulations are carried out utilizing the LAMMPS software package[22] CVFF[23] was used to calculate bonding and non-bonding interactions. The force-field distribution have accurately predicted thermodynamic properties of components in our system[24]. The details of MD simulations can be found in the supporting information.

Preprints (www.preprints.org) | NOT PEER-REVIEWED | Posted: 25 October 2017 doi:10.20944/preprints201710.0162.v1

Peer-reviewed version available at Polymers 2017, 9, 688; doi:10.3390/polym9120688

2.5 Scanning electron microscope (SEM)

The PAAm hydrogels with different crosslinking density were freeze-dried to keep their original microstructures before analyzed by SEM (FEI, Helios) with an accelerating voltage at 2.0 kV.

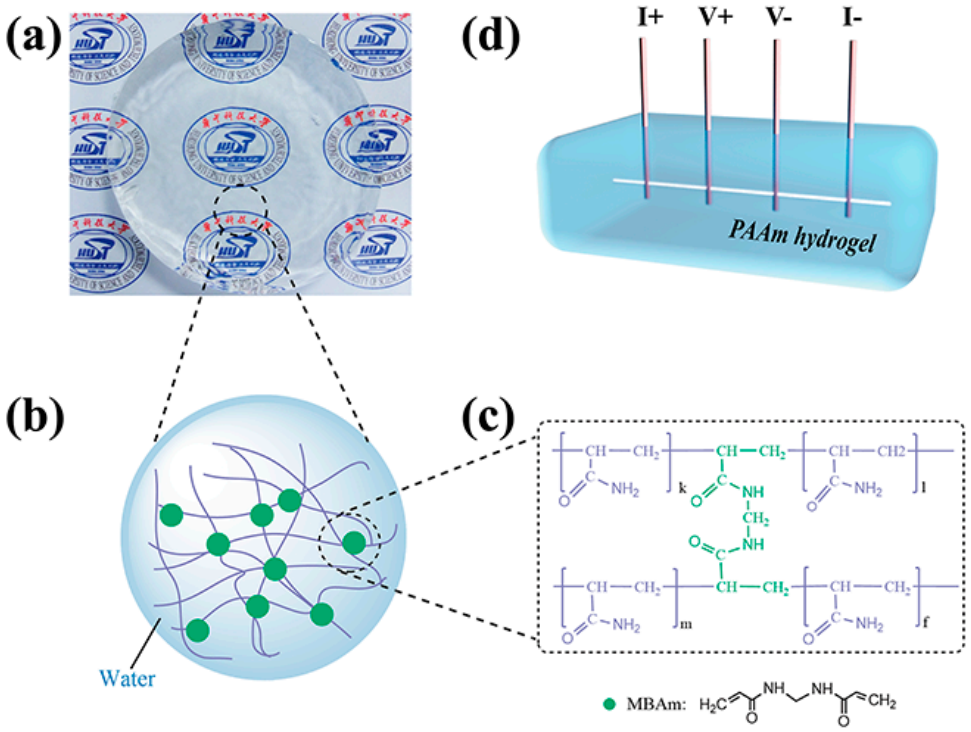

Figure 1. PAAm hydrogel and its experimental setup for thermal conductivity measurement. (a) Optical image of the as-prepared PAAm hydrogel sample. (b) Schematic of the polymer network with covalent crosslinking through MBAm (green circles.). (c) The molecular structures of the covalently crosslinked polymer chains. (d) The Schematic illustration of 3ωmethod setup for thermal conductivity measurement of hydrogels. A platinum wire is deeply immersed in hydrogels and wired out with four copper probes for applied current and voltage measurements. The four brown rods are copper probes and the white line in hydrogel is the Pt wire.

3. Results and Discussion

Various technologies have been developed to measure thermo-physical properties of materials in different states and conditions, such as laser-flash method, 3ω method, steady-state method, and etc. When it comes to hydrogels samples, which is unique for their intrinsic half-liquid and half-solid characteristics, it is challenging and special consideration is needed. For example, laser-flash method is a simple one and has been reported to measure thermal conductivity of hydrogel nanocomposites with BN nanosheets[19]. But laser-flash method usually requires opaque samples and thus is not appropriate for the completely transparent samples. 3ω method is chosen here because 3ω method has shown to be successful in measuring samples in liquid[25,26], in addition to bulk[27] and thin film samples[28].

The thermal conductivities of PAAm hydrogels as a function of crosslinker concentrations measured by 3ω method are shown in the blue curves in Figure 2a. At the low crosslinker concentration range of 0.016 to 0.099 mol %, the thermal conductivity of hydrogels increases fast and

almost linearly from 0.33±0.06 to 0.51±0.03 $Wm^{-1}K^{-1}$, giving a 54% enhancement. With the crosslinker concentration further increases to 0.263 mol %, the thermal conductivity decreases to 0.33±0.04 W/m-K. All the thermal conductivities of hydrogels measured in our experiments are below 0.60 $Wm^{-1}K^{-1}$. This means, the thermal conductivity of hydrogels consisting of crosslinked polymer network with significant amount water seems always below that of pure water. We assume that the intrinsic thermal behaviors of hydrogels are tightly related to their effective crosslinking density and polymer backbones. The concept was further validated by equilibrium swelling experiment SEM characterization at first.

To obtain the effective crosslinking density in PAAm hydrogels and understand the corresponding thermal transport behaviors, we implemented equilibrium swelling experiment firstly. The water will be imbibed into the polymer network and stretch the polymer chains when the hydrogels are soaked in water. Figure 2b presents the time dependent swelling weight of PAAm hydrogels with different crosslinker concentrations. The weight of the hydrogels increases fast at first and will reach saturation when hydrogels are in their equilibrium state after a few days' swelling. As shown in Figure 2c, the corresponding calculated effective crosslinking density increases fast in the crosslinker concentrations range of 0.016 to 0.099 mol%, and increases slowly when the concentration increases to 0.263 mol %. This result indicates that adding more MBAm into PAAm hydrogels tend to higher crosslinking degree in our work. Detailed analysis of this measurement is included in supporting information.

As shown in Figure 2d-f, SEM images of the freeze-dried PAAm hydrogel samples reveal that gels with lower (0.033mol%) cross-linker concentration exhibit discrete leaflet structures, indicating a low crosslinking degree of the polymer network. The ordered honeycomb-like structure was found in PAAm hydrogels with higher cross-linker (0.099mol% and 0.263 mol%), showing significantly enhanced crosslinking degree. The decreased pore size in the honeycomb structure (Figure 2f) implies a more compact structure as a result of higher degree of crosslinking density.

In amorphous polymer, previous studies have revealed that the effective crosslinking density will basically affect thermal conductivity in two ways[29,30]. On one hand, the addition of covalent crosslinking bonds will increase thermal conduction pathways between prior non-bonded chain segments, which is verified by the SEM images in Figure 2d-f. On the other hand, more crosslinking bonds will introduce more phonon scattering along the backbone chains, which reduces the phonon mean free path. Particularly, when the crosslinking density is low (0~10 mol %), the two effects will cancel each other[29,30]. For large crosslinking density (10~80 mol %), the increase of thermal conduction pathway dominates, which poses a linear increase in thermal conductivity. In our case, when the crosslinking density is very small (0.016~0.099 mol %), the enhancement of thermal conductivity could be attributed to the transition from weak van der Waals interactions to strong covalently bonding interactions, which multiplies the thermal transport pathways. While crosslinking network grows (crosslinker concentration 0.099~0.263 mol %), the amount of side chain increases as well which brings in more phonons scattering effect. The two competitive mechanisms lead to the variations of thermal conductivity in PAAm hydrogel, as shown in Figure 2a.

Preprints (www.preprints.org) | NOT PEER-REVIEWED | Posted: 25 October 2017 doi:10.20944/preprints201710.0162.v1

Peer-reviewed version available at Polymers 2017, 9, 688; doi:10.3390/polym9120688

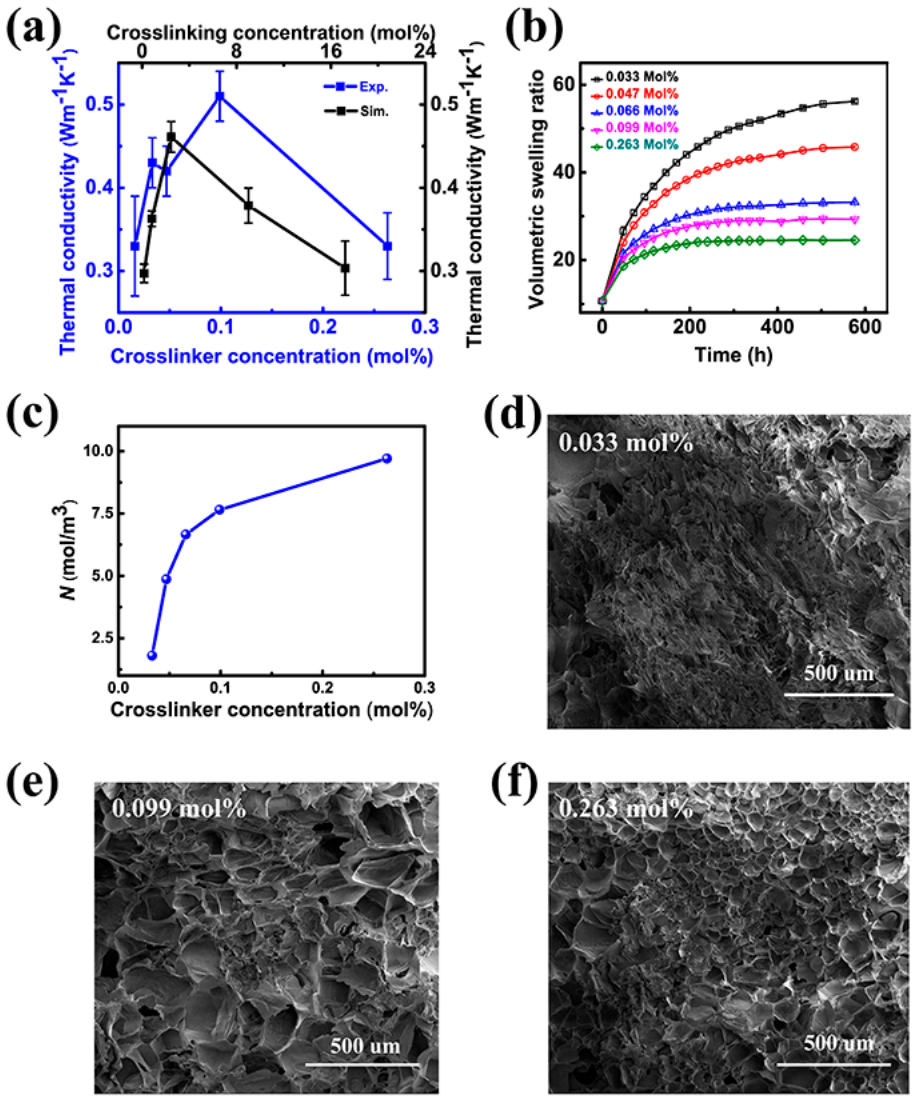

Figure 2. Crosslinking effect of PAAm hydrogels. (a) Experimental and simulation results on the thermal conductivity of PAAm hydrogels with different crosslinker concentrations. The blue curves are the experimentally measured thermal conductivities by 3ω method, and the black curves are the simulated thermal conductivities by molecular dynamics simulations. (b) The volumetric swelling ratio of PAAm hydrogels as a function of swelling time. (c) The relationship of the effective crosslinking density, N, and the corresponding crosslinker concentration. SEM images of PAAm gels of constant monomer concentrations and different stages of cross-linking: (d) 0.033 mol%; (e) 0.099 mol%; (f) 0.263 mol%.

In order to quantitatively study the thermal conductivity of covalently crosslinked PAAm, EMD simulations based on Green-Kubo method are performed. Simulation details and the theory are shown in Figure S4 (Supplementary Information). A similar trend of descending after rising in thermal conductivity with crosslinking concentration is observed in our EMD simulation as shown in the black curves in Figure 2a. In EMD simulation, amorphous PAAm chains crosslinked by MBAm are modeled without considering water effect. Actually, the sufficient water content in hydrogels may contribute significantly to the thermal conduction behaviors of the half-solid and half-liquid samples, which can be inferred from the fact that our EMD simulated results are smaller than the experimental ones.

Preprints (www.preprints.org) | NOT PEER-REVIEWED | Posted: 25 October 2017 doi:10.20944/preprints201710.0162.v1

Peer-reviewed version available at Polymers 2017, 9, 688; doi:10.3390/polym9120688

Therefore, we further investigate the thermal conduction behaviors of PAAm hydrogels as a function of water content. To change the water content in PAAm hydrogel while preserving the original conformation at the same time, ethanol solution is used to dry the hydrogels to obtain samples with different water fractions. As shown in Figure 3a, the thermal conductivity increases gradually from 0.41±0.04 to 0.46±0.03 $Wm^{-1}K^{-1}$ as the water fraction increase from 23 wt% to 79 wt%. The thermal conductivity of hydrogel containing 88 wt% water reaches 0.57±0.04 $Wm^{-1}K^{-1}$, which is a little bit below that of pure water (0.60 $Wm^{-1}K^{-1}$). With water permeated into the polymer backbone, polymer chains in hydrogel could be stretched. In polymer system, stretching is an effective method to enlarge thermal conductive property in polymer system because of the accompanied better chain alignment and less defects[18,31,32]. The thermal conductivity of the drawn nanofibers could be as high as 104 $Wm^{-1}K^{-1}$. The behind physical mechanism for the thermal transportation in hydrogels involving crosslinking network and water is complicated requires far more efforts from both experimental and theoretical studies. It will be interesting if we treat hydrogels as pure water containing cross-linked polymer network. As the fraction of polymer network increases from 0% to 70%, the thermal conductivity will keep decreasing from 0.60 $Wm^{-1}K^{-1}$ to a relatively low value, like 0.41 $Wm^{-1}K^{-1}$. The addition of the cross-linked polymer network will destroy the thermal conduction pathways in pure water.

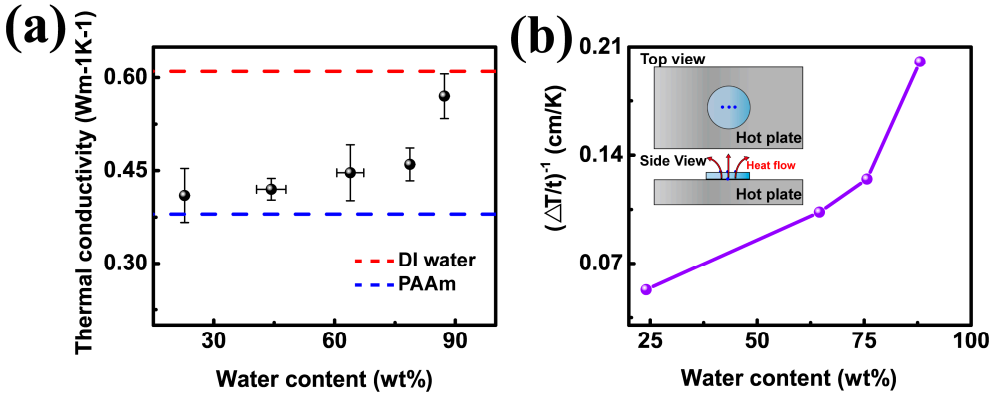

Figure 3. Demonstration of the thermal conductivity of the PAAm hydrogel with 0.099 mol% crosslinker and different water content. (a) 3ω based measurement for thermal conductivity of PAAm hydrogels with varied water content. (b) Heat dissipation ability with change of water content. Inset: Illustration of measurement of heat dissipation for PAAm hydrogels. The blue dots represent thermocouples. Three thermocouples are put on the surface of sample with distance of about 2 mm between each other, and the another one is under the bottom of hydrogel. Temperature gradient come from the difference between the value of the bottom thermocouple and the average value of the three top thermocouples in the equilibrium state.

The effect of water content on the thermal conductivity of hydrogels is also investigated by measuring heat dissipation curves. Hydrogel samples are cut into a 10 mm thick disk and placed on a 60 °C hot plate at room temperature of 25 °C, as presented in the inset of Figure 3b. The temperature on top surface of the sample is monitored as a function of time by three thermal couples. Heating continues until samples reach their temperature balance state. Figure 3b presents the plot $(\Delta T/_t)^{-1}$ as a function of water content, which is in good agreement with Figure 3a. Because the thermal conductivity is inversely proportional to the thickness normalized temperature difference, $\kappa \propto (\Delta T/_t)^{-1}$.

Since human body is mainly made of hydrogels, the thermal conduction behaviors of hydrogels at different temperature are potentially important, for example human body in a fever state. Thus we evaluate the thermal behavior of PAAm hydrogel in a temperature range of 25~40 °C. We find that hydrogel is insensitive to temperature in this temperature range and exhibits neither deterioration nor enhancement as shown as Figure 4.

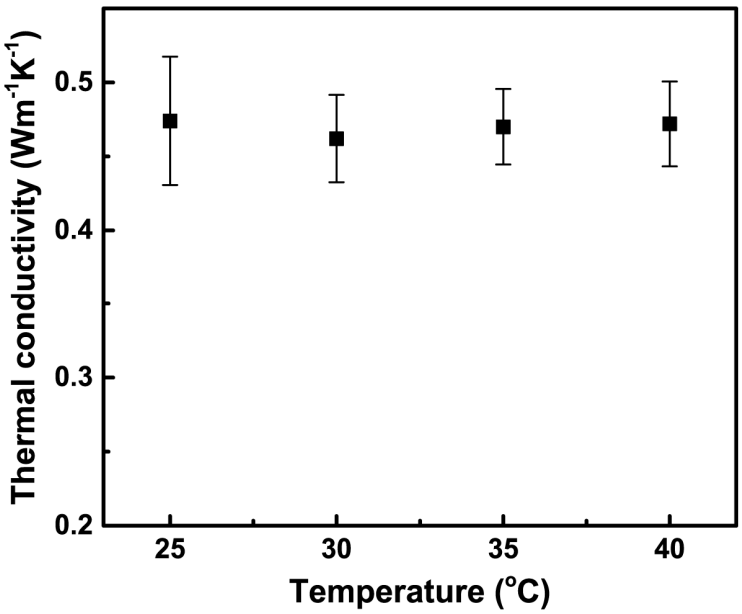

Figure 4. Temperature dependent thermal conductivity of PAAm hydrogels with crosslinker amount of 0.099 mol% measured by 3ω method.

Finally, we demonstrate the heat dissipation behaviors of the hydrogel with a heat source inside the sample through IR thermal imaging camera. As shown in Figure 5a and 5b, an electrically heated graphite rod is plugged through the PAAm hydrogel block (0.51 $Wm^{-1}K^{-1}$) to provide a heat source and the thermal camera records the time dependent temperature distribution on the top view of samples. Figure 5c presents the heat propagates radically from the heat source to the outer circles, generating a 10℃ temperature gradient in a distance of 10 mm within 8 min.

Peer-reviewed version available at Polymers 2017, 9, 688; doi:10.3390/polym9120688

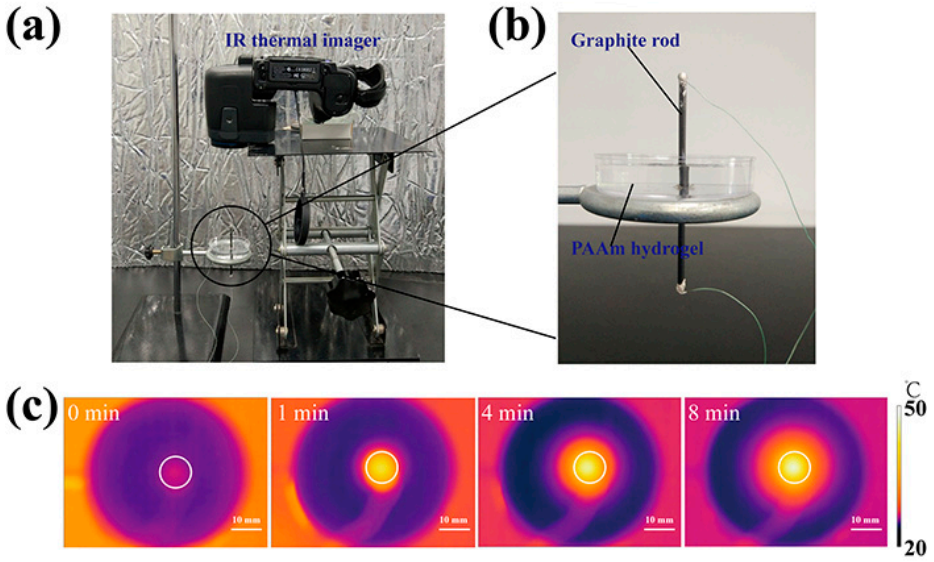

Figure 5. A demonstration of heat dissipation behaviors in the hydrogel by IR thermal imaging camera. (1) Optical image of the whole measurement system. The IR thermal camera is fixed on top of the hydrogel sample to record the thermal change. (b) Optical image of the sample. An electrically heated graphite rod is plugged through the PAAm hydrogel sample with crosslinker amount of o.099 mol%. (c) IR thermal images of the hydrogel at different heating time.

4. Conclusions

In summary, the thermal conductivity of PAAm hydrogels has been experimentally measured using 3ω method. The variation of the thermal conductivity is in a range of 0.33 ~ 0.51 $Wm^{-1}K^{-1}$ by tuning the crosslinking density. The increase of crosslink bonding between the polymer chains will favor thermal conduction by increasing conduction pathways at the cost of bringing in more phonon scattering effect. The competition mechanism is further supported by the equilibrium swelling ratio measurement, SEM characterization and molecular simulation analysis. Besides crosslinking density effect, thermal conductivity of hydrogel is also dependent on its water fraction related as well. From 23 wt% to 88 wt% of water content, thermal conductivity can be modulated between 0.41 and 0.57 $Wm^{-1}K^{-1}$. It's interesting that over 50% change of thermal conduction of PAAm hydrogel could be achieved only by adjusting its crosslinking density and water content, without adding any fillers like nanosheets of graphene or boron nitride. More research efforts regarding the effect of bonding type, polymer chain alignment and porous structure are expected to devote in the future to better understand the thermal conduction behaviors in hydrogels. Our study offers an attempt towards understanding of thermal transport in soft materials, and may be beneficial to the design of hydrogel-based devices.

Supplementary Information: The following are available online at www.mdpi.com/link, Figure S1: Picture of 3-ω method experimental setup; Figure S2: Experimental data for sample with 0.033wt% crosslinker concentration at room temperature 295.1K; Figure S3: Schematic of 3ωmeasurement for different water content and temperature dependent thermal conduction in PAAm hydrogels; Figure S4: Molecular dynamics simulation cell setup and one example of data analysis.

Acknowledgements: This work was supported by the National Natural Science Foundation of China

No. 51572096 (J. Z.) and No. 51576076 (N. Y.), and the National 1000 Talents Program of China tenable in HUST (J. Z.).

Author Contributions: Jianfeng Zang and Nuo Yang conceived and designed the experiments and simulations. Ni Tang, Zhan Peng and Rulei Guo performed the experiments. Meng An conducted the simulations. Xiandong Chen and Xiaobo Li contributed to the measurement method. All authors analyzed data.

Conflicts of Interest: The authors declare no conflict of interest.

References

1. Gerlach G, A. K. F. *Hydrogel Sensors and Biosensors*, Springer, Berlin 2010.
2. Lutolf, M. P.; Hubbell, J. a. Synthetic Biomaterials as Instructive Extracellular Microenvironments for Morphogenesis in Tissue Engineering. *Nat. Biotechnol.* 2005, 23 (1), 47–55.
3. Tibbitt, M. W.; Anseth, K. S. Hydrogels as Extracellular Matrix Mimics for 3D Cell Culture. *Biotechnol. Bioeng.* **2009**, *103* (4), 655–663.
4. Peppas, N. A.; Hilt, J. Z.; Khademhosseini, A.; Langer, R. Hydrogels in Biology and Medicine: From Molecular Principles to Bionanotechnology. *Adv. Mater.* **2006**, *18* (11), 1345–1360.
5. Calvert, P. Hydrogels for Soft Machines. *Adv. Mater.* **2009**, *21* (7), 743–756.
6. Gong, J. P.; Katsuyama, Y.; Kurokawa, T.; Osada, Y. Double-Network Hydrogels with Extremely High Mechanical Strength. *Adv. Mater.* **2003**, *15* (14), 1155–1158.
7. Sun, J.-Y.; Zhao, X.; Illeperuma, W. R. K.; Chaudhuri, O.; Oh, K. H.; Mooney, D. J.; Vlassak, J. J.; Suo, Z. Highly Stretchable and Tough Hydrogels. *Nature.* **2012**, *489* (7414), 133–136.
8. Zhao, X. Multi-Scale Multi-Mechanism Design of Tough Hydrogels: Building Dissipation into Stretchy Networks. *Soft Matter.* **2014**, *10* (5), 672–687.
9. Li, J.; Suo, Z.; Vlassak, J. J. Stiff, Strong, and Tough Hydrogels with Good Chemical Stability. *J. Mater. Chem. B.* **2014**, *2* (39), 6708–6713.
10. Hong, S.; Sycks, D.; Chan, H. F. ai; Lin, S.; Lopez, G. P.; Guilak, F.; Leong, K. W.; Zhao, X. 3D Printing: 3D Printing of Highly Stretchable and Tough Hydrogels into Complex, Cellularized Structures. *Adv. Mater.* **2015**, *27* (27), 4034.
11. Kim, C.-C.; Lee, H.-H.; Oh, K. H.; Sun, J.-Y. Highly Stretchable, Transparent Ionic Touch Panel. *Science.* **2016**, 353 (6300), 682–687.
12. Selvaraj, M., Takahata, K. A Steerable Smart Catheter Tip Realized by Flexible Hydrogel Actuator. In *In 2016 IEEE 29th International Conference on Micro Electro Mechanical Systems (MEMS).* IEEE, Shanghai, China, January 2016.
13. Guo, J.; Liu, X.; Jiang, N.; Yetisen, A. K.; Yuk, H.; Yang, C.; Khademhosseini, A.; Zhao, X.; Yun, S. H. Highly Stretchable, Strain Sensing Hydrogel Optical Fibers. *Adv. Mater.* **2016,** 28(46), 10244.
14. Sun, Y.; Zhou, X.; Liu, Y.; Zhao, G.; Jiang, Y. Effect of Magnetic Nanoparticles on the Properties of Magnetic Rubber. *Mater. Res. Bull.* **2010**, *45* (7), 878–881.
15. Koob, T. J.; Hernandez, D. J. Mechanical and Thermal Properties of Novel Polymerized NDGA-Gelatin Hydrogels. *Biomaterials.* **2003**, *24* (7), 1285–1292.
16. Dash, R.; Foston, M.; Ragauskas, A. J. Improving the Mechanical and Thermal Properties of Gelatin Hydrogels Cross-Linked by Cellulose Nanowhiskers. *Carbohydr. Polym.* **2013**, *91* (2), 638–645.
17. Othman, M. B. H.; Md Akil, H.; Md Rasib, S. Z.; Khan, A.; Ahmad, Z. Thermal Properties and Kinetic

Investigation of Chitosan-PMAA Based Dual-Responsive Hydrogels. *Ind. Crops Prod.* **2015**, *66*, 178–187.

18. Zaragoza, J.; Babhadiashar, N.; O'Brien, V.; Chang, A.; Blanco, M.; Zabalegui, A.; Lee, H.; Asuri, P. Experimental Investigation of Mechanical and Thermal Properties of Silica Nanoparticle-Reinforced Poly(acrylamide) Nanocomposite Hydrogels. *PLoS One.* **2015**, *10* (8), 1–11.
19. Xiao, F.; Naficy, S.; Casillas, G.; Khan, M. H.; Katkus, T.; Jiang, L.; Liu, H.; Li, H.; Huang, Z. Edge-Hydroxylated Boron Nitride Nanosheets as an Effective Additive to Improve the Thermal Response of Hydrogels. *Adv. Mater.* **2015**, *27* (44), 7196–7203.
20. Jiang, H.; Wang, Z.; Geng, H.; Song, X.; Zeng, H.; ZHI, C. Highly Flexible and Self-Healable Thermal Interface Material Based on Boron Nitride Nanosheets and a Dual Cross-Linked Hydrogel. *ACS Appl. Mater. Interfaces.* **2017**, 9(11), 10078-10084.
21. Xu, X.; Pereira, L. F. C.; Wang, Y.; Wu, J.; Zhang, K.; Zhao, X.; Bae, S.; Tinh Bui, C.; Xie, R.; Thong, J. T. L.; Hong, B. H.; Loh, K. P.; Donadio, D.; Li, B.; Özyilmaz, B. Length-Dependent Thermal Conductivity in Suspended Single-Layer Graphene. *Nat. Commun.* **2014**, *5*, 3689.
22. Plimpton, S. Fast Parallel Algorithms for Short-Range Molecular Dynamics. *Journal of Computational Physics*. 1995, 117(1), 1-19.
23. Victoria, P. D.; David, A. R.; Wolff, J.; Genest, M. Structure and Energetics of Ligand Binding to Proteins : Escherichia coZi Dihydrofolate Reductase-Trimethoprim , A Drug-Receptor System. *Protein-structure Funct. Bioinforma.* **1988**, *47*, 31–47.
24. Varshney, V.; Patnaik, S. S.; Roy, A. K.; Farmer, B. L. Heat Transport in Epoxy Networks: A Molecular Dynamics Study. *Polymer (Guildf).* **2009**, *50* (14), 3378–3385.
25. Yusibani, E.; Woodfield, P. L.; Fujii, M.; Shinzato, K.; Zhang, X.; Takata, Y. Application of the Three-Omega Method to Measurement of Thermal Conductivity and Thermal Diffusivity of Hydrogen Gas. *Int. J. Thermophys.* **2009**, *30* (2), 397–415.
26. Oh, D. W.; Jain, A.; Eaton, J. K.; Goodson, K. E.; Lee, J. S. Thermal Conductivity Measurement and Sedimentation Detection of Aluminum Oxide Nanofluids by Using the 3ω Method. *Int. J. Heat Fluid Flow.* **2008**, *29* (5), 1456–1461.
27. Cahill, D. G.; Katiyar, M.; Abelson, J. R. Thermal-Conductivity of Alpha-SiH Thin-Films. *Phys. Rev. B.* **1994**, 50, 6077-6081.
28. Cahill, D. G. Thermal Conductivity Measurement from 30 to 750 K: The 3ω Method. *Rev. Sci. Instrum.* **1990**, *61* (2), 802–808.
29. Ni, B.; Watanabe, T.; Phillpot, S. R. Thermal Transport in Polyethylene and at Polyethylene-Diamond Interfaces Investigated Using Molecular Dynamics Simulation. *J. Phys. Condens. Matter* **2009**, *21* (8), 84219.
30. Kikugawa, G.; Desai, T. G.; Keblinski, P.; Ohara, T. Effect of Crosslink Formation on Heat Conduction in Amorphous Polymers. *J. Appl. Phys.* **2013**, *114* (3), 034302-034302-6.
31. Shen, S.; Henry, A.; Tong, J.; Zheng, R.; Chen, G. Polyethylene Nanofibres with Very High Thermal Conductivities. *Nat. Nanotechnol.* **2010**, *5* (4), 251–255.
32. Ma, J.; Zhang, Q.; Mayo, A.; Ni, Z.; Yi, H.; Chen, Y.; Mu, R.; Bellan, L. M.; Li, D. Thermal Conductivity of Electrospun Polyethylene Nanofibers. *Nanoscale.* **2015**, *7* (40), 16899–16908.